



ELSEVIER

Contents lists available at ScienceDirect

Computers &amp; Fluids

journal homepage: [www.elsevier.com/locate/compfluid](http://www.elsevier.com/locate/compfluid)

## Time-scale joint representation of DNS and LES numerical data

Guy Courbebaisse<sup>a</sup>, Roland Bouffanais<sup>b,\*</sup>, Laurent Navarro<sup>c</sup>, Emmanuel Leriche<sup>d</sup>, Michel Deville<sup>e</sup>

<sup>a</sup> Université de Lyon, CREATIS-LRMN, CNRS UMR5220, INSERM U630, INSA-Lyon, Université Lyon 1, INSA-Bâtiment Blaise Pascal, 7 avenue Jean Capelle, F-69621 Villeurbanne cedex, France

<sup>b</sup> Massachusetts Institute of Technology, Department of Mechanical Engineering, 77 Massachusetts Avenue, Bldg 5-326, Cambridge, MA 02139, USA

<sup>c</sup> CIS, École Nationale Supérieure des Mines de Saint-Étienne, 158 Cours Fauriel, F-42023 Saint-Étienne, France

<sup>d</sup> Université de Saint-Étienne, 23 rue Docteur Paul Michelon, F-42023 Saint-Étienne Cedex 2, France

<sup>e</sup> STI-IGM-LIN, École Polytechnique Fédérale de Lausanne, Station 9, CH-1015 Lausanne, Switzerland

### ARTICLE INFO

#### Article history:

Received 7 May 2010

Received in revised form 7 August 2010

Accepted 7 September 2010

Available online 21 September 2010

#### Keywords:

Direct numerical simulation

Large-eddy simulation

Wavelet analysis

Time-scale joint representation

Lid-driven cavity flow

### ABSTRACT

A spectral analysis and a multiscale study are performed on the numerical data obtained from direct numerical simulation and large-eddy simulation of the turbulent flow in a cubical lid-driven cavity. The analyzed data or signals are picked at three specific points inside the cavity allowing to investigate three drastically different flow regimes over time: laminar, transitional and turbulent. In comparison with direct numerical simulation, large-eddy simulation not only have a reduced resolution in space but also in time. In this context a wavelet analysis is chosen to study signals from large-eddy simulation, to provide a 'local' analysis of transient turbulent events. A time-scale joint representation is generated by continuous wavelet transform and compared with the time-scale joint representation of the direct numerical simulation. In this framework, the main objective of this study is to confirm the correlation between the computed physical quantities and those expected theoretically.

© 2010 Elsevier Ltd. All rights reserved.

### 1. Introduction

The analysis of sampled signals obtained from experiments and direct numerical simulation (DNS) of turbulent fluid flows through wavelet analysis is now common practice. Such analysis often provides tremendous insight into the flow behavior otherwise difficult, if not impossible, to apprehend with more conventional statistical signal analysis methods (e.g. Fourier transform). The use of wavelet analysis to study signals from large-eddy simulation (LES) is not as common, mainly because of the intrinsic high level of non-physical noise introduced by the subgrid models and the reduced resolution both in space and in time. However, depending on the subgrid model and the numerical method used, these difficulties may be overcome.

After a brief description of the main features of the lid-driven cubical cavity flow, the characteristic parameters are provided for both DNS and LES methods of simulation. Then the choice of the three analyzed points within the cavity is motivated and the coordinates of the three points are specified. After a classical spectral validation (sampled condition), a multiscale approach based on wavelet transform provides a relevant analysis of signals consider-

ing the three regimes, namely laminar, transitional and turbulent. Such an approach has been employed and is reported here for the study of the time histories of the pressure and other fluctuating quantities in the locally-turbulent regime of the lid-driven cubical cavity flow; the main objective being to confirm the correlation between the computed physical quantities and those expected theoretically.

### 2. The lid-driven cubical cavity flow

The flow field contained within a cubical enclosure (see Fig. 1) is generated by imposing a motion of the 'top' wall's cavity (with the velocity vector being everywhere parallel to the  $x$ -axis). On the remaining five sides homogeneous no-slip conditions are enforced. The two faces normal to the  $x$ -axis will be referred to as downstream and upstream, depending of their positions relatively to the motion of the lid, whereas the faces normal to the  $z$ -axis will be referred to as side walls. The remaining face parallel to the moving lid will be called the bottom wall. The three-dimensional domain of the flow is defined on  $[-h, +h]^3$ . The center of the axes system is assigned to the center of the cavity. This places the boundaries of the flow domain at  $\pm h$  of each axis. This problem is known as the lid-driven cavity (LDC) problem. Even though the problem statement appears fairly simple, the physical nature of the resulting flow regimes is known to be very complex and

\* Corresponding author.

E-mail addresses: [guy.courbebaisse@creatis.insa-lyon.fr](mailto:guy.courbebaisse@creatis.insa-lyon.fr) (G. Courbebaisse), [bouffana@mit.edu](mailto:bouffana@mit.edu) (R. Bouffanais), [navarro@emse.fr](mailto:navarro@emse.fr) (L. Navarro), [emmanuel.leriche@univ-st-etienne.fr](mailto:emmanuel.leriche@univ-st-etienne.fr) (E. Leriche), [michel.deville@epfl.ch](mailto:michel.deville@epfl.ch) (M. Deville).

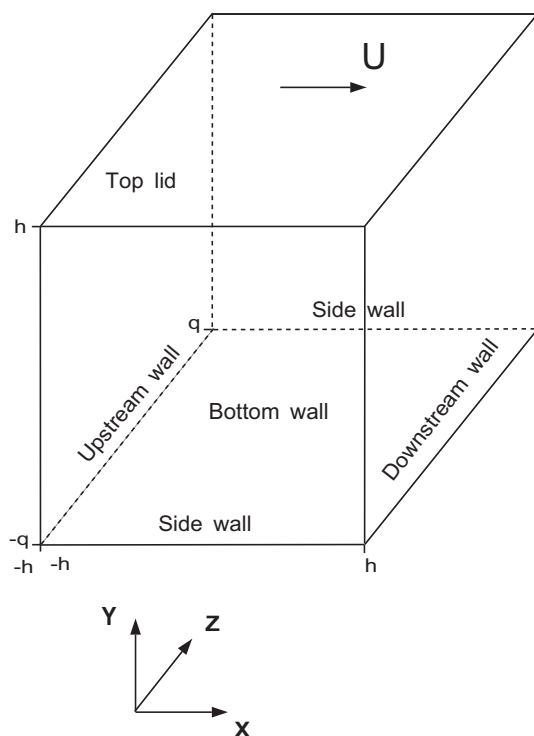


Fig. 1. Sketch of the geometry of the lid-driven cubical cavity.

deserve to be analyzed in many details. The fluid enclosed in the cavity is assumed to be incompressible, Newtonian with constant physical properties throughout its volume. The equation of motion for the fluid inside the cavity is given by the Navier–Stokes equations. The flow of a viscous Newtonian incompressible fluid within a lid-driven cavity is an idealization of a number of fluid mechanics problems. From a physical point of view, several well-known flow phenomena appear in the LDC like shear flow, boundary layers, eddies and core vortex, and, with the occurrence of curved streamlines, a contribution due to the associated (Görtler) instability mechanism to the dynamics of the flow, Taylor–Görtler-like vortices. Less well known aspects of this flow concern the presence of streaks near the moving wall, of jet impingement at the walls, and of corner spiraling vortices and at high Reynolds number, the coexistence of adjacent regions of laminar and turbulent flow within the cavity [1–3].

Specific features of lid-driven cavity flows in the turbulent regime, such as inhomogeneity of turbulence, turbulence production near the downstream-corner-eddy, small-scales localization and helical properties have been investigated and discussed in direct and large-eddy simulations framework [1–3]. Time histories of quantities such as the total energy, total turbulent kinetic energy or helicity exhibit different evolutions but only after a relatively long transient period. At a Reynolds number of 12,000, the lid-driven cavity flow is in the locally-turbulent regime and is proved to be highly inhomogeneous in the secondary-corner regions of the cavity where turbulence production and dissipation are important [1–3]. The maximum production of turbulence is located at the downstream wall jet impingement point, just above the bottom wall, nearby the downstream-corner-eddy region.

In [1–3], the mean momentum budgets are presented and the leading terms in these balances are examined. The Reynolds stress budgets are computed and the statistics for the distribution of energy between the various components are discussed. Moreover, the effects of Reynolds number on the driven cavity flow are briefly addressed.

### 3. Direct numerical simulation of the lid-driven cubical cavity flow

The direct numerical simulation (DNS) of the LDC flow involves the solution of the full transient, nonlinear Navier–Stokes equations without any modeling of turbulence. DNS provides thus a complete description of a turbulent flow, and the instantaneous flow variables (e.g. velocity and pressure) are known as a function of space and time. The DNS resolves all dynamically important turbulence scales, from the largest and most energetic generating eddies, down to the smallest dissipative Kolmogorov scales.

Direct numerical simulation of the flow in a lid-driven cubical cavity has been carried out at a Reynolds number (based on the maximum velocity on the lid), of 12,000. The resolution used up to 2.1 ( $129^3$ ) million Chebyshev collocation nodes, which enables the detailed representation of all dynamically significant scales of motion. The main numerical parameters of the DNS of the LDC flow at a Reynolds number of 12,000 are presented in Table 1.

The spatial approximation of the equations of motion (i.e. the incompressible Navier–Stokes equations) is based on the standard Chebyshev collocation method based on Gauss–Lobatto quadrature rules [4], which consists of exactly enforcing the differential equations, and the boundary conditions at the Chebyshev–Gauss–Lobatto points. It is based on the use of tensor product expansions in Chebyshev polynomials of order  $N$  along every space direction. This high-order method eliminates diffusion and dispersion errors in the solution – the latter being common with low-order methods (e.g. finite difference methods or low-order finite element methods) currently used in three-dimensional numerical simulations of bounded flows. All matrices arising from the discretization are cast into the tensor product form with substantial gains in computational efficiency.

### 4. Large-eddy simulation of the lid-driven cubical cavity flow

Large-eddy simulation of the turbulent flow in a lid-driven cubical cavity have been carried out at the same Reynolds number, i.e. 12,000, as for the DNS but using the Legendre spectral element method [3,5]. Two distinct subgrid-scales models, namely a dynamic Smagorinsky model (DSM) and a dynamic mixed model (DMM), have been both validated *a priori* and implemented *a posteriori* to perform long-lasting simulations required by the relevant time-scales of the flow. The resolution in time is high enough so that subgrid modeling is only needed to account for the reduced resolution in space. Practically, it is usually more cost-effective to be under-resolved in space than in time. In addition, being under-resolved both in space and time leads to unavoidable numerical instabilities, e.g. Courant–Friedrich–Lewy (CFL) criterion not respected, etc. All filtering levels make use of explicit filters applied in the physical space (on an element-by-element approach) and spectral (modal) spaces to separate the resolved (“large”) scales from the modeled (“small”) ones. The two subgrid-scales models had been validated and compared to available experimental and numerical reference results, showing very good agreement.

Table 1

Main numerical parameters for the direct and large-eddy simulation of the LDC flow at Reynolds number 12,000:  $K$  is the number of Legendre spectral elements in each spatial direction,  $N$  is the degree of Chebyshev (resp. Legendre) polynomials in each spatial direction for the DNS (resp. LES),  $\Delta t$  is the time step, and the associated sampling time with which the instantaneous velocity and pressure fields have been stored.

	$K$	$N$	$\Delta t$	Sampling
DNS	–	128	$2.5 \times 10^{-3}$	0.25
LES	8	8	$2.0 \times 10^{-3}$	0.6

The Legendre spectral element method (SEM) is a high-order spatial discretization method for the approximate Galerkin solution of Navier–Stokes equations expressed in weak variational forms [5]. The SEM relies on the division of the cavity domain into conforming elements within each one, every velocity flow variable is expanded in tensor-product Lagrange interpolants (polynomial of order  $N$  in every space direction) based on  $(N + 1)$  Gauss–Lobatto–Legendre points in conjunction with particular quadrature rules. Like high-order finite element techniques, the SEM can deal with arbitrary complex geometry where  $h$ -refinement is achieved by increasing the number of spectral elements and  $p$ -refinement by increasing the Lagrangian polynomial order within the elements. The SEM brings the exponential rate-of-convergence associated with high-order precision combined with the geometrical flexibility of finite elements. From a high-order precision standpoint, the SEM is comparable to spectral methods as an exponential rate-of-convergence is observed when smooth solutions to regular problems are sought. Velocity  $C^0$ -continuity across element interfaces requires the exact same interpolation in each and every spectral element sharing a common interface but the continuity of the first derivative is reached in the weak sense. Continuity of all derivative orders across element boundaries is attained in the limit  $N \rightarrow \infty$ . Moreover, to prevent any spurious pressure modes in the Navier–Stokes computations, the choice of a staggered  $\mathbb{P}_N - \mathbb{P}_{N-2}$  interpolation method for the velocity and pressure respectively, has been made [6,7].

The main numerical parameters of the LES of the LDC flow at a Reynolds number of 12,000 are presented in Table 1 with  $K = 8$  number of Legendre spectral elements, and  $N = 8$  for the degree of the Legendre polynomials in each spatial direction. When removing the redundant points at the elements interfaces, the total number of degrees of freedom (dof) is  $65^3$ , representing 1/8 of the total dof used by the DNS.

### 5. The three selected probed points

Three points have been carefully and purposely selected inside the cavity with a location corresponding to three drastically different flow states. At these three selected points, for the DNS and LES-DSM respectively, velocity, pressure and kinetic energy instantaneous signals have been recorded over 1200 (resp. 1000) dimensionless time units with a sampling of 100 time steps (resp. 300 time steps), in accordance with the sampling time given in Table 1. For the LES, only the resolved part have been used and the analysis of the signals are performed with those coming from LES-DSM, the LES-DMM signals analysis providing the same quantitative results. For consistency reasons, DNS data have been down-sampled with a ratio of 2.4, hence leading to the same sampling rate as the LES data.

The point  $P_1$  is located in a laminar region at the center of the cavity with coordinates:

$$P_1 = \left( \frac{x_1}{h} = 0.0, \frac{y_1}{h} = 0.0, \frac{z_1}{h} = 0.0 \right). \quad (1)$$

The point  $P_2$  is located in a transitional region near the downstream wall jet (which is highly unsteady) with coordinates:

$$P_2 = \left( \frac{x_2}{h} = 0.6155, \frac{y_2}{h} = -0.6122, \frac{z_2}{h} = -0.6021 \right). \quad (2)$$

The point  $P_3$  is located in a region where the mean turbulence production reaches its maximum due to the jet impingement and where a large amount of small-scales structures are present. Its coordinates are:

$$P_3 = \left( \frac{x_3}{h} = 0.7874, \frac{y_3}{h} = -0.9388, \frac{z_3}{h} = -0.3371 \right). \quad (3)$$

The time history of the instantaneous turbulence production recorded in the region of this maximum of the mean turbulence

production exhibits relatively few very high peaks [1,3]. The peaks obtained by the LES have lower intensity in comparison with those obtained by DNS due to the filtered scales of the LES. For both DNS and LES, those peaks (or clusters of them) show a minimum separation in time of about 100 dimensionless time. The conditional average of the instantaneous velocity field according to a prescribed threshold value provides the associated coherent structure: a pair of counter-rotating vortices. Due to the filtering separation of the resolved (“large”) eddies from the modeled or filtered (“small”) ones, it is expected that all LES signals will exhibit less behavior coming from the small-scales.

### 6. Spectral analysis

The time series of the three considered quantities, namely pressure, local kinetic energy and  $x$ -component of the velocity field, have been extracted from the DNS and LES databases at the three distinct locations inside the cavity introduced in Section 5. Fig. 2 presents the pressure and the velocity signals issued from DNS and LES simulations. Each probed point has been purposely chosen to characterize the three different regimes – laminar, transitional, turbulent – encountered within the lid-driven cavity flow at  $Re = 12,000$  as discussed in Section 5. The groundbreaking work of Kolmogorov [8] highlights the fact that the velocity fluctuations of a turbulent flow can be analyzed and characterized based upon the behaviors of the scales of the spatial increment of the Eulerian velocity or the temporal increment of the Lagrangian velocity. The central postulate of statistical isotropy of small spatial and temporal scales, used by Kolmogorov in [8] is directly connected to the independence of these small-scales with respect to the mechanism of injection of energy which occurs at the large scales through the formation of the large eddies. In addition, the statistical analysis of the temporal fluctuations of the pressure field allows one to study the vortically-intense regions of the flow [1]. Given the fact that the pressure field is the solution of a Poisson equation (the flow being incompressible), the vortical structures are therefore connected to the rapid changes in the temporal signal of the pressure field, see Fig. 2.

A pre-analysis of the simulated system consists in the Fourier transform computation applied to the velocity signal and to the pressure signal at the point  $P_3$  of maximum mean turbulence production within the cavity. The Fourier transform can be written as [9]:

$$S(v) = \int s(t)e^{-2i\pi vt} dt, \quad (4)$$

where  $s(t)$  is the analyzed signal,  $t$  the time and  $v$  the frequency.

The results of the spectral analysis for the intensity (square modulus of the quantity) in a Log-Log scale are shown in Fig. 3 (resp Fig. 4) where a  $-5/3$  (resp.  $-7/3$ ) slope is observed for the velocity (resp. pressure) signals. These results which are characteristics of the developed turbulence region of the cavity flow are in good agreement with those predicted by the statistical theory of the turbulence K41 [8]. Slopes were conventionally estimated using a linear regression method. It is worth noting that these spectra (as well as the subsequent ones in this article) lack smoothness at high frequencies due to the limited size of our databases of turbulent flow samples. It must be added that nowadays, the storage of these databases represents a serious practical issue, if not a bottleneck, in the production of DNS databases [2].

In order to get a meaningful spectral analysis, the sampling period should be compatible with the Shannon’s theorem [9]. The Nyquist frequency being higher than the maximum frequency of the DNS and LES signals, no aliasing error are found, as shown in Fig. 5.

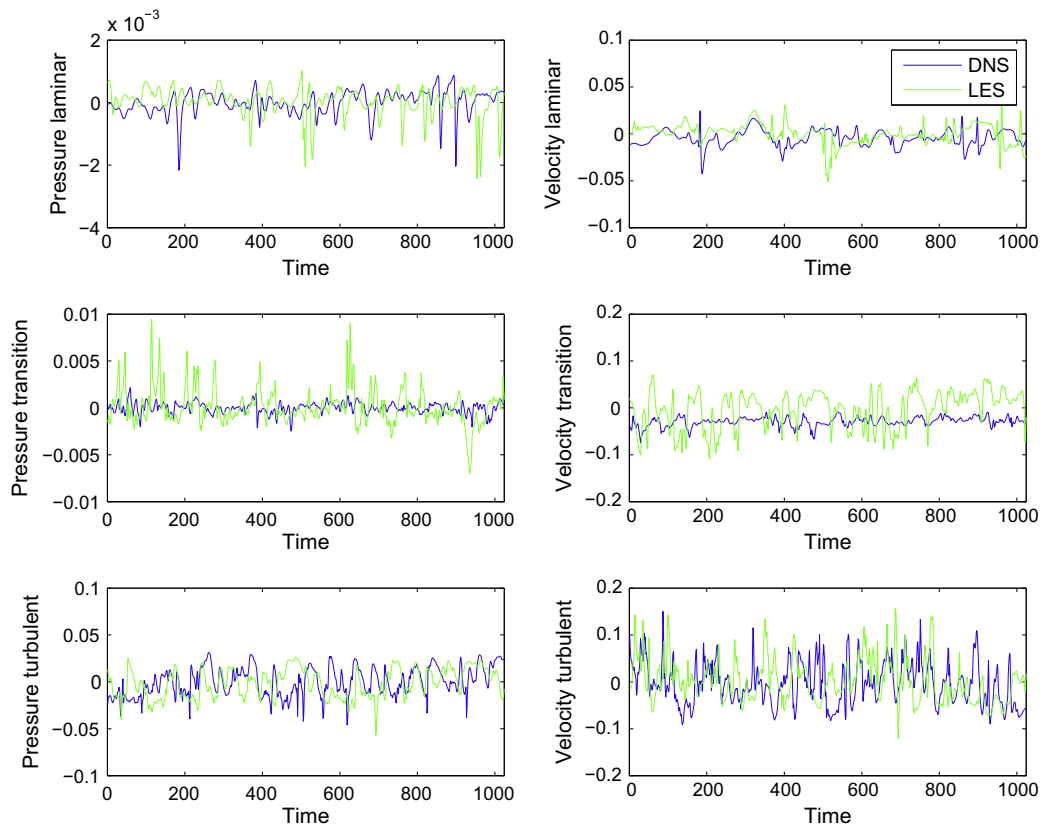


Fig. 2. Pressure fields and velocities for the three regimes for DNS and LES simulations.

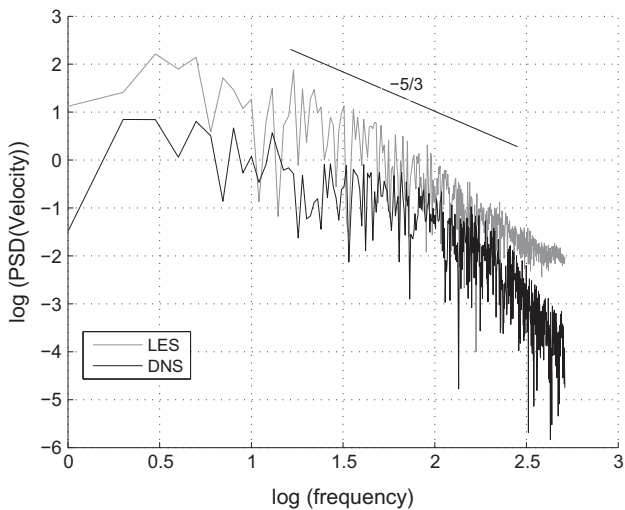


Fig. 3. Fourier transforms of the time histories of the DNS and LES velocity signals at the point  $P_3$  of maximum mean turbulence production within the cavity.

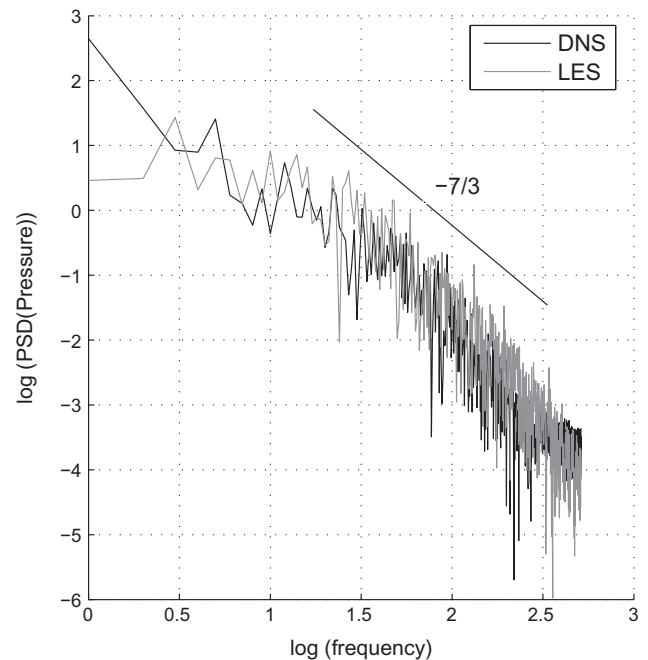


Fig. 4. Fourier transform of the time histories of the DNS and LES pressure signals at the point  $P_3$  of maximum mean turbulence production within the cavity.

### 7. Wavelet transform and wavelet transform modulus maxima analysis

The simple and traditional spectral (Fourier) analysis presented in Section 6 provides interesting initial results. However, such spectral analysis is known to provide limited insight.

More advanced signal analyses of turbulent data have been reported in the literature and, without being exhaustive, it is worth mentioning two specific techniques. First, a multiscale geometric analysis has been reported in [10], in which the curvelet transform

is used. The curvelet transform is an extension of the wavelet transform concept using polar coordinates). It is applied in [10] to the total vorticity of both experimental and DNS signals of a turbulent flow, with the aim to reconstruct the two- and three-dimensional coherent vortical structures. Second, a hybrid method

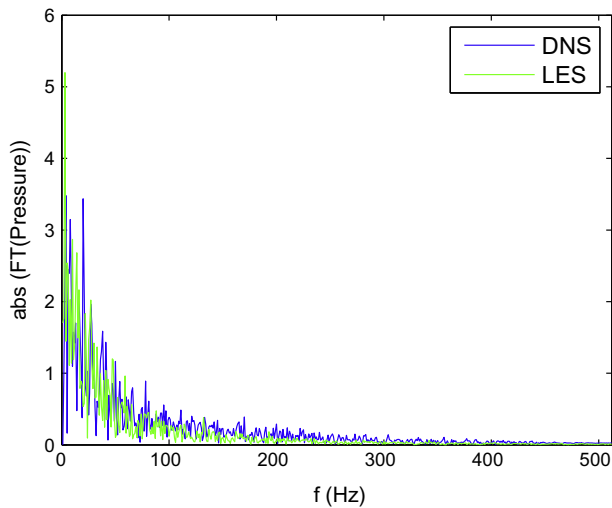


Fig. 5. Fourier transform of the time histories of the DNS and LES pressure signals at the point  $P_3$  of maximum mean turbulence production within the cavity.

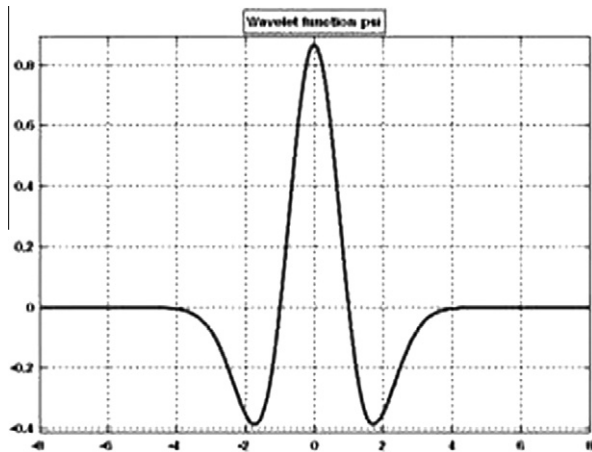


Fig. 6. Mexican hat wavelet.

is introduced in [11], where a proper orthogonal decomposition (POD) technique is coupled to multiscale wavelet analysis and applied to experimental PIV data for the analysis of some specific flow structures and their time evolution. The wavelet transform is both used for denoising the PIV data and also to obtain scale wise decomposition (discrete wavelet transform) of the POD modes in order to study spatial topologies of the considered turbulent flows.

In the present work, we aim at finding the most appropriate signal analysis allowing to characterize the turbulent coherent struc-

tures (large eddies) simulated by a LES, in comparison to those obtained of the associated DNS and obtained by CVE [12]. As a second step, a continuous wavelet transform (CWT) analysis is considered [9,13]. The CWT is known to be well suited to investigate signals generated by turbulent phenomena [9,14].

The continuous wavelet transform is expressed by

$$C_\psi[s](a, b) = \langle \Psi_{a,b}, s \rangle = \int \overline{\Psi_{a,b}}(t) s(t) dt, \quad (5)$$

with

$$\Psi_{a,b} = \frac{1}{\sqrt{a}} \Psi\left(\frac{t-b}{a}\right), \quad (6)$$

and corresponds to the inner product of the signal  $s(t)$  with the successive versions of the mother wavelet  $\Psi_{a,b}$ , where  $a$  is a real positive parameter and  $b$  a real parameter, and the overline denotes the complex conjugate. The selected wavelet must verify the following admissibility condition  $\int \Psi(t) dt = 0$ . In the sequel, all wavelet analyses are based on the so-called ‘‘Mexican hat’’ wavelet (Fig. 6) expressed by

$$\Psi(t) = \frac{2\pi^{-1/4}}{\sqrt{3}} (1 - t^2) e^{-t^2/2}. \quad (7)$$

The choice of the wavelet leads to the second derivative of the Gaussian function (see Fig. 6). In fact this wavelet is  $C^\infty$  and is well localized in the time domain as in the frequency domain. In addition, its two first moments vanish and verify

$$\int x^q \Psi(t) dt = 0, \quad 0 \leq q < 2. \quad (8)$$

This property is essential analyzing singularities within a signal [14].

The continuous wavelet transform  $C_\psi[s](a, b)$  is now a conventional tool for the analysis of singularities in a signal at an instant  $t_0$ , and hence allows one to expand the concept of ‘singularity exponent’. It is well-known that the wavelet transform, near a singular point  $b = t_0$ , behaves like a power law according to the scale with the Hölder exponent  $h(t_0)$ , namely:  $|C_\psi[s](a, t_0)| \propto a^{h(t_0)}$ . The Hölder exponent  $h(t_0)$  is a measure of the strength of the singularity [14,15].

In the present work, given the (inhomogeneous) production of turbulence within the cavity flow [3,1], a multi-resolution analysis of signals extracted from the DNS and LES database appears like a promising strategy. The results of the wavelet transform computation are traditionally presented in a graph with a horizontal axis for the time, a vertical one for the scale  $a$  and flooded color contours of the continuous wavelet transform. The continuous wavelet transform of the DNS and LES signals are used to reveal the changing patterns between the three regimes, laminar, transitional and turbulent. The wavelet analysis of the pressure signal is shown in Figs. 7 and 8. Fig. 8 highlights the gradual emergence of LES ‘time-scale’

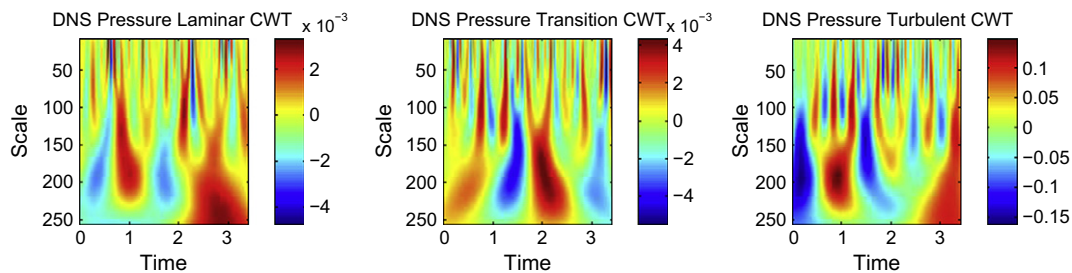
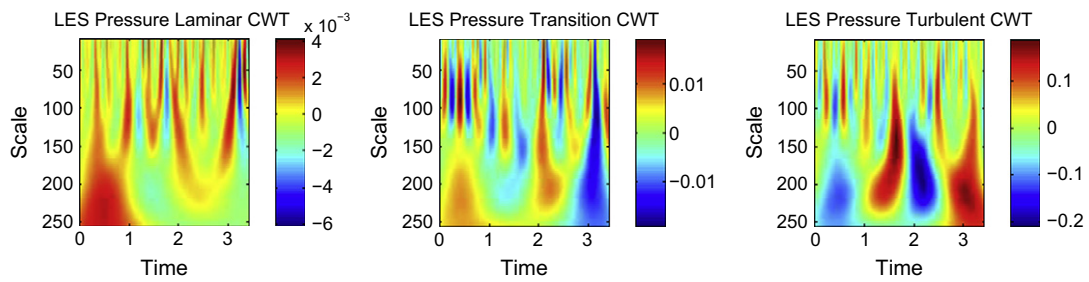
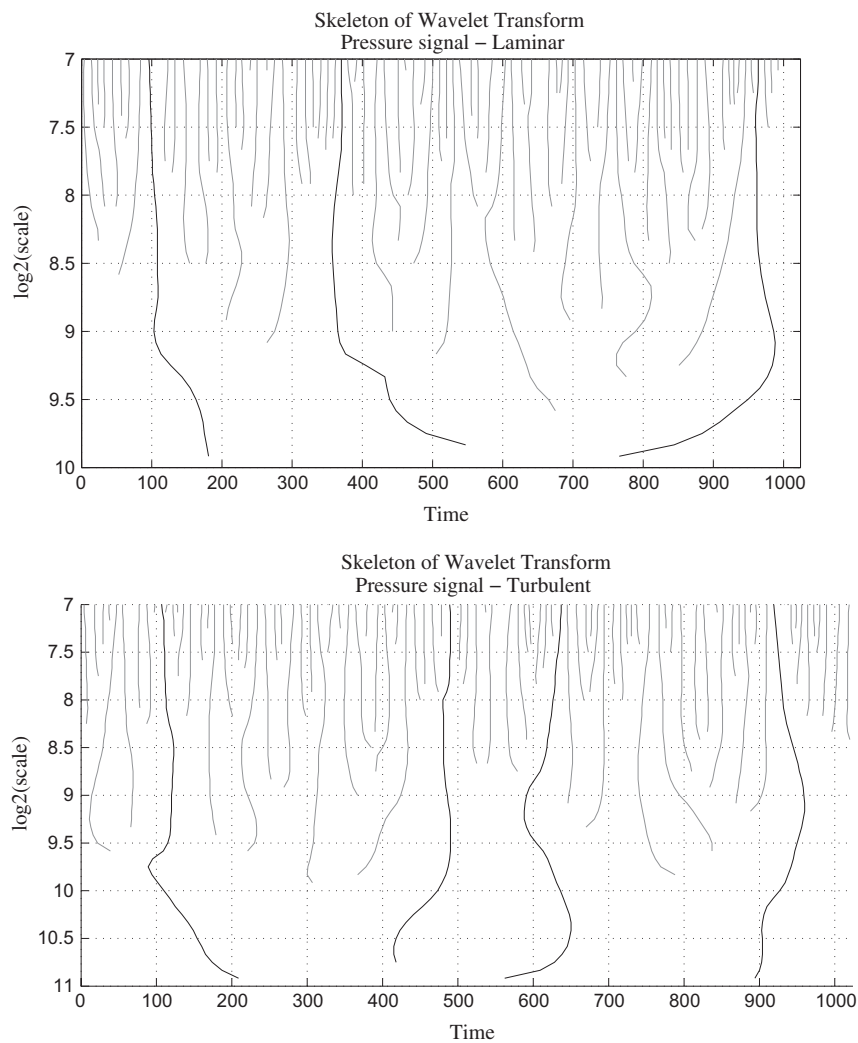


Fig. 7. Continuous wavelet transform of the DNS pressure field at the three locations of the cavity corresponding to laminar, transitional and turbulent regimes. Red (resp. blue) represents positive (resp. negative) contour levels. (For interpretation of the references to color in this figure legend, the reader is referred to the web version of this article.)



**Fig. 8.** Continuous wavelet transform of the LES pressure field at the three locations of the cavity corresponding to laminar, transitional and turbulent regimes. Red (resp. blue) represents positive (resp. negative) contour levels. (For interpretation of the references to color in this figure legend, the reader is referred to the web version of this article.)



**Fig. 9.** Skeleton of the wavelet transform of the LES pressure field successively for both the laminar (top) and turbulent (bottom) regimes.

patterns at large scales. As expected in the DNS simulation all the scales of eddies contribute to the generated turbulence and Fig. 7 provides a representation of the turbulence across all scales.

To quantify the turbulence, it seems relevant to implement the wavelet transform modulus maxima analysis (WTMM) [14]. In particular, the skeleton (defined by the lines of maxima of the wavelet transform modulus) is calculated for the pressure signal in both laminar and turbulent regimes. The results are shown in Fig. 9 where filaments appear for both the laminar and the turbulent cases. The longest filaments are collected and represented in

Fig. 10 where the scale is on the horizontal axis and the magnitude of the filaments on the vertical one. The laminar filaments appear almost constant in amplitude, whereas the filaments for the turbulent regime display a  $-2/3$  slope. This  $-2/3$  slope corresponds to very large depressions associated with the turbulent bursts occurring when a pair of counter-rotating vortices is produced [3,1]. The identified singularities are very strong and have a negative Hölder exponent. The above results for the turbulent region of the flow provide structures possessing a clear fractal signature, which is also related to the high level of singularities. In addition,

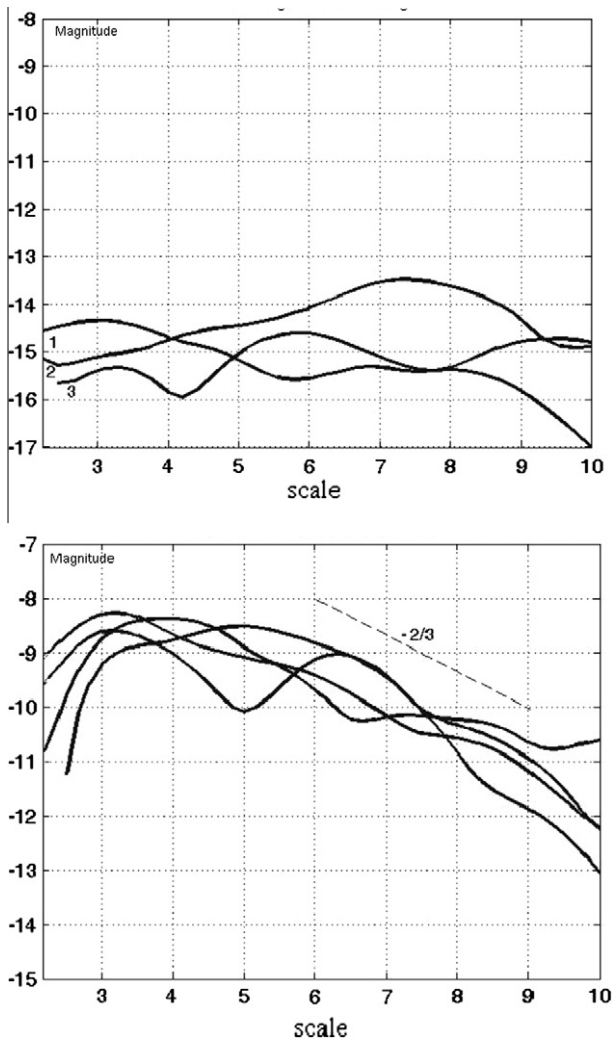


Fig. 10. Amplitude of the wavelet transform along the longest filaments of the skeleton of the LES pressure field successively for both the laminar (top) and turbulent (bottom) regimes.

when considering the DNS case, the calculated skeleton behavior for the pressure signal for the turbulent regime, hence reinforcing our discussion in the LES case. The results are shown in Fig. 11

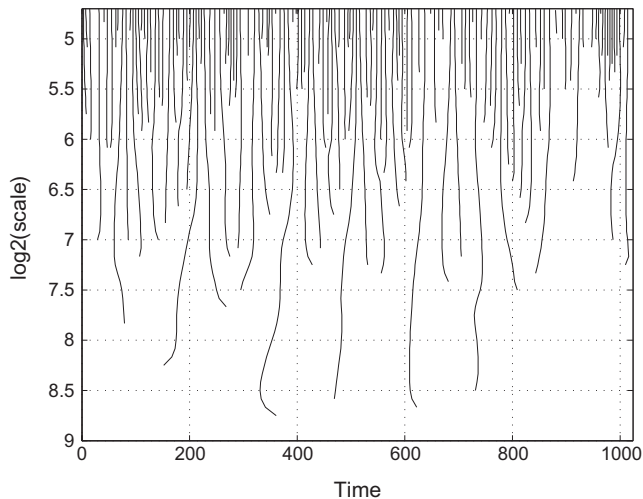


Fig. 11. Skeleton of the wavelet transform of the DNS pressure field in the turbulent regime.

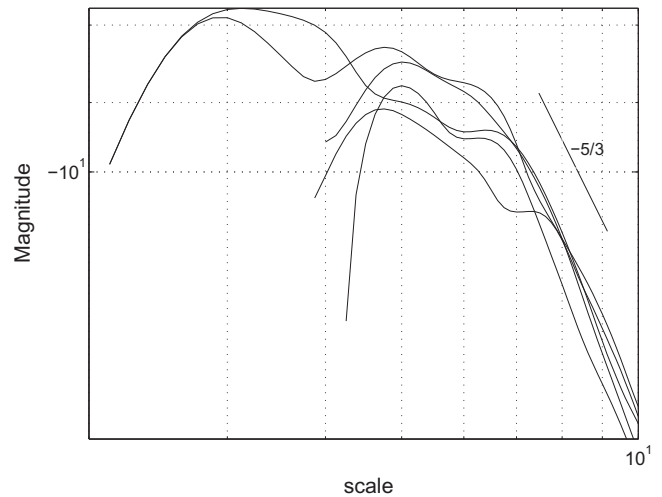


Fig. 12. Amplitude of the wavelet transform of the DNS pressure field along the longest filaments of the skeleton in the turbulent regime.

where filaments appear highlighting a high level of singularities and in Fig. 12 where a  $-5/3$  slope measurement is linked to turbulence scales and to the interaction between small and large eddies.

### 8. WTMM method and spectrum of singularities

To characterize the DNS and LES signals, one has to resort to a multi-fractal model and hence study the spectrum of Hölder exponent, also known as ‘spectrum of singularities’. Considering a multi-fractal formalism [16,15], the K41 theory [8] leads to a statistical homogeneous velocity field characterized by only one Hölder exponent when the Reynolds number tends to infinity. For small scales, the properties of invariance of the Navier–Stokes equations are statistically preserved. However, when considering intermittency phenomena in fluid flow, the assumption of homogeneity is no longer valid for small-scales. An improvement of the earlier statistical theory of homogeneous and isotropic turbulence K41 [8] is given by the K62 [17,18] theory which allows one to consider intermittent phenomena. Similarity assumptions (statistical relation between local fluctuations of the velocity field and fluctuations of the dissipative energy field) in the case of isotropic turbulence can be understood from the multi-fractal formalism [9,14–16].

Furthermore to achieve a better computation of the spectrum of singularities, we should consider a longer time integration for the DNS and the LES – the database sampling time turned out to be accurate –, up to several thousand dimensionless time. The present DNS and LES simulation span only for 1000 dimensionless time, and increasing the total dimensionless time will be rather expensive for DNS, but may be feasible. Moreover, to study the statistical distribution of singularities, it is necessary to calculate the spectrum of singularities  $D(h)$  by a multi-fractal formalism based on the wavelet transform modulus maxima method (WTMM) [14].

### 9. Conclusions

Continuous wavelet transform coupled to WTMM analysis, is implemented to analyze DNS and LES signals in order to characterize the locally turbulent flow in a lid-driven cubical cavity. Despite the inherently low space and time resolution of the LES signals, the wavelet analysis reveals some very interesting features through its Hölder exponent in a multi-fractal framework. In addition, the wavelet transforms of DNS and LES signals deliver representations

highlighting the specificities of DNS and LES. Comparisons of these results for three different locations within the cavity corresponding to three different flow regimes show the effectiveness of this approach for a locally inhomogeneous and anisotropic flow such as the one in the lid-driven cavity at a Reynolds number of 12,000. At this step, a more general investigation and characterization of physical quantities computed through DNS and LES in other flow configurations is suggested.

### Acknowledgments

The DNS data were obtained on supercomputing facilities at the Swiss National Supercomputing Center CSCS and the LES data on Pleiades cluster at EPFL-ISE.

It is a genuine pleasure to dedicate this paper to Michel Deville on the occasion of his retirement; his continuous support and guidance have been invaluable and immensely enriching and have led to the current fruitful collaboration among all the authors.

### References

- [1] Leriche E, Gavrilakis S. Direct numerical simulation of the flow in the lid-driven cubical cavity. *Phys Fluids* 2000;12:1363–76.
- [2] Leriche E. Direct numerical simulation of lid driven cavity at high Reynolds numbers by a Chebyshev spectral method. *SIAM J Sci Comput* 2006;27:335–45.
- [3] Bouffanais R, Deville MO, Leriche E. Large-eddy simulation of the flow in a lid-driven cubical cavity. *Phys Fluids* 2007;19. doi:10.1063/1.2723153 [Art. 055108].
- [4] Canuto C, Hussaini MY, Quarteroni A, Zang TA. *Spectral methods – fundamentals in single domains*. New York: Springer Verlag; 2006.
- [5] Deville MO, Fischer PF, Mund EH. *High-order methods for incompressible fluid flow*. Cambridge, UK: Cambridge University Press; 2002. doi:10.1017/CBO9780511546792.
- [6] Maday Y, Patera AT. Spectral element methods for the incompressible Navier–Stokes equations. In: Noor AK, Oden JT, editors. *State-of-the-art survey on computational mechanics*. New York: ASME; 1989. p. 71–142.
- [7] Maday Y, Patera AT, Rønquist EM. The  $\mathbb{P}_N \times \mathbb{P}_{N-2}$  method for the approximation of the Stokes problem, Tech. Rep. 92009. Cambridge, MA: Department of Mechanical Engineering, MIT; 1992.
- [8] Kolmogorov AN. The local structure of turbulence in incompressible viscous fluid for very large Reynolds numbers. *CR Acad Sci USSR* 1941: 299–303.
- [9] Mallat S. *A wavelet tour of signal processing*. 2nd ed. Academic Press; 1999.
- [10] Ma JW, Hussaini MY, Vasilyev OV, Le Dimet F-X. Multiscale geometric analysis of turbulence by curvelets. *Phys Fluids* 2009;21. doi:10.1063/1.3177355 [Art. 075104].
- [11] Tabib MV, Sathe MJ, Deshpande SS, Joshi JB. A hybridized snapshot proper orthogonal decomposition-discrete wavelet transform technique for the analysis of flow structures and their time evolution. *Chem Eng Sci* 2009;64:4319–40. doi:10.1016/j.ces.2009.06.025.
- [12] Kadoch B, Leriche E, Schneider K, Farge M. On the role of coherent structures for a lid driven cavity flow. In: Deville M, Lê TH, Sagaut M, editors. *Notes on numerical fluid mechanics and multidisciplinary design*, vol. 110. Berlin: Springer Verlag; 2010. p. 207–14.
- [13] Carmona R, Hwang WL, Torrèsani B. *Practical time-frequency analysis*. Academic Press; 1997.
- [14] Arneodo A, Argoul F, Bacry E, Elezgaray J, Muzy JF. *Fractales. Ondelettes et Turbulence : de l'ADN aux croissances cristallines*. Diderot Editions; 1995.
- [15] Jaffard S. Multifractal formalism for functions. Part 1 and 2. *SIAM J Math Anal* 1997;28:944–98.
- [16] Frisch U. *Turbulence: The legacy of AN Kolmogorov*. Cambridge, UK: Cambridge University Press; 1995.
- [17] Kolmogorov AN. A refinement of previous hypotheses concerning the local structure of turbulence in a viscous incompressible fluid at high Reynolds number. *J Fluid Mech* 1962;13:82–5.
- [18] Obukhov OM. Some specific features of atmospheric turbulence. *J Fluid Mech* 1962;13:77.